Modeling, Simulation and Control of a 4WD Electric Vehicle with In-Wheel Motors

R. Iervolino[*], **A. Sakhnevych**[†]

[*]Dipartimento di Ingegneria Elettrica e delle Tecnologie dell'Informazione, Università degli Studi di Napoli, Federico II, Via Claudio 21, 80125 Napoli, Italy, email: rafierv@unina.it

[†]Dipartimento di Ingegneria Industriale, Università degli Studi di Napoli, Federico II, Via Claudio 21, 80125 Napoli, Italy, email: aleksandr.sakhnevych@unina.it

Abstract. A relatively new technology for the electric vehicles considers the use of brushless permanent magnet motors directly connected to the car wheels (*in-wheel motors* or *hub motors*). In order to evaluate the performance that can be obtained, a complete dynamic model of a four-wheel drive (4WD) electric vehicle equipped with four in-wheel motors is developed and a correspondent parametric simulator is implemented in Matlab/Simulink™. The simulator is also employed for designing, testing and comparing various control logics which reproduce the handling behavior of a real vehicle.

Keywords: In-wheel motors, Virtual simulation and control, Model in the Loop, Vehicle dynamics, Differential logics.

1 Introduction

In the last years, several car manufacturers have focused their efforts on the production of completely electric vehicles with the aim of both increasing the energy efficiency and reducing the environmental impact [1, 2].

A step forward in this direction is offered by the introduction of a new technology based on electric motors directly connected to the wheels (also known as *in-wheel motors* or *hub motors*) [3, 4]. The best suited electric motor class for the inclusion in the wheel rims is represented by the permanent magnet brushless DC motors, thanks to their compactness, low weight, high torque per unit mass and volume, and maximum speed. The adopted solutions are many, because, without the need of any transmission shafts, traction can be moved from the front to the rear axle almost arbitrarily. As a result, the four-wheel drive (4WD) should be easily achieved [5]. Moreover, independently controlled motors allow high dynamic performance, without the presence of complex gearboxes and mechanical differentials. The price is an increased complexity in the control design algorithms, considering also the negative effects of augmented unsprung mass on vehicle performance dynamics [6, 7].

In this paper, a complete vehicle, wheel and tire dynamic model is built, with the inclusion of the electric in-wheel motors. The mathematical model is then implemented in a modular and parametric simulator by using the Matlab/Simulink™ environment. The simulator is employed both for the analysis of the system performance and the synthesis of robust control algorithms [8, 9, 10].

The paper is organized as follows: in Section 2, some preliminaries about the overall system mathematical model are recalled; in Section 3 the simulator is described in detail and the most significant simulation results are reported; in Section 4 some differential control logics, related to the torque distribution among the in-wheel motors, are analyzed and compared. Finally, Section 5 concludes the paper.

2 Preliminaries

In this Section, some preliminaries about the vehicle dynamic modeling are synthetically recalled. The global mathematical model is obtained by assembling the models of the system main components: vehicle, tires, in-wheel motors.

2.1 Vehicle dynamics

There exist numerous mathematical models in literature for representing the vehicle dynamics. If the interest is limited to its directional behavior, with the hypothesis of slowly varying forward speed, the bounce and the pitch motions of the car body can be neglected [11]. By further assuming long-range and low-speed turns, the roll degree of freedom can be also disregarded. As a consequence, a planar model is considered for the vehicle rigid body dynamics.
Other simplifying assumptions are:

- the wheels mass is negligible;
- the vehicle is moving on a flat and rigid road, such as to be considered a geometrical plane;
- there is a univocal relationship between the steering wheel angle and the wheel angle;
- the steering axis is vertical and passes through the center of the contact.

The car body reference system has the x-axis parallel to the ground, in the forward direction, the z-axis orthogonal to the road plan and upwards directed, and the y-axis to complete the left-handed reference frame.

By referring to Fig. 1, with the hypothesis of small angles, the congruence equations are:

$$\alpha_{1s} = \delta - \frac{v + ra_1}{u - rt/2} , \qquad (1)$$

$$\alpha_{1D} = \delta - \frac{v+ra_1}{u+rt/2}, \quad (2)$$

$$\alpha_{2s} = -\frac{v-ra_2}{u-rt/2}, \quad (3)$$

$$\alpha_{2D} = -\frac{v-ra_2}{u+rt/2}, \quad (4)$$

where t is the car track width; a_1 is the front wheelbase; a_2 is the rear wheelbase; u is the forwarding speed; v is the lateral speed; δ is the steering angle; r is the yaw rate; $\alpha_{1s}, \alpha_{1D}, \alpha_{2s}, \alpha_{2D}$ are the slip angles.

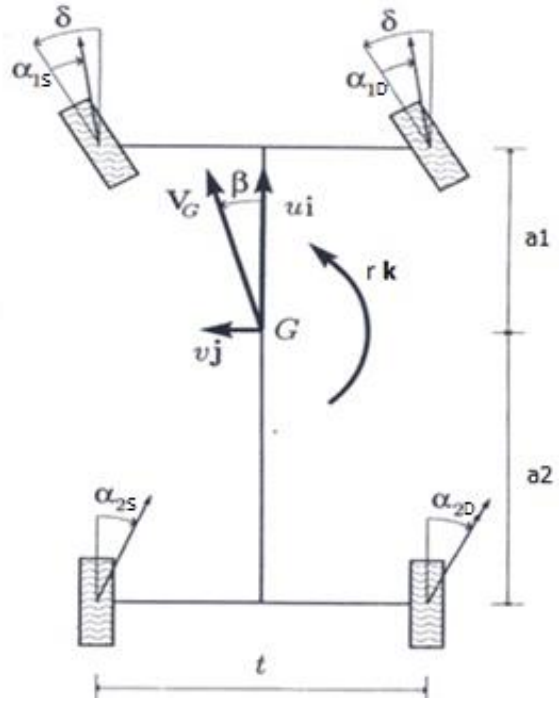

Fig. 1 Kinematic quantities definition**.**

The equations of motions can be expressed by using the classical rigid body dynamics equations. By referring to the force and torque scheme of Fig. 2, the model is:

$$m \cdot (\dot{u} - vr) = X = (F_{x1s} + F_{x1d}) \cdot \cos(\delta) + F_{x2s} + F_{x2d} - (F_{y1s} + F_{y1d}) \cdot \sin(\delta) - \frac{1}{2}\rho C_x S u^2, \quad (5)$$

$$m \cdot (\dot{v} + ur) = Y = (F_{y1s} + F_{y1d}) \cdot \cos(\delta) + (F_{x1s} + F_{x1d}) \cdot \sin(\delta) + F_{y2s} + F_{y2d}, \quad (6)$$

$$J\dot{r} = N = (F_{y1s} + F_{y1d}) \cdot a_1 \cdot \cos(\delta) - (F_{y2s} + F_{y2d}) \cdot a_2 + (F_{x1s} + F_{x1d}) \cdot a_1 \cdot \sin(\delta) - \frac{t}{2} \cdot [(F_{x1s} - F_{x1d}) \cdot \cos(\delta) + (F_{x2s} - F_{x2d}) - (F_{y1s} - F_{y1d}) \cdot \sin(\delta)]. \quad (7)$$

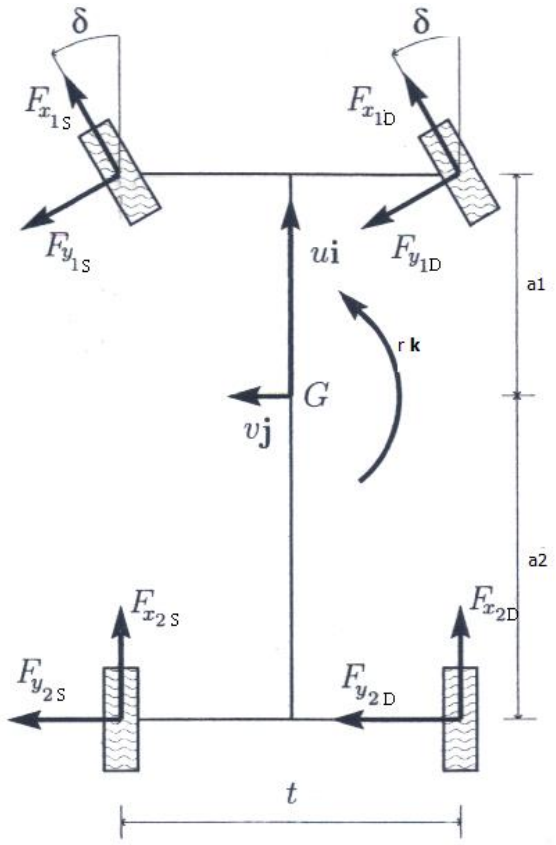

Fig. 2 Forces acting on the vehicle.

2.2 Tire model

The interaction force between the tire and the road can be described by using the well-known and widely employed Pacejka "Magic Formula" [12]:

$$\mathrm{Y(x)} = \mathrm{D} \cdot \cos\{\mathrm{C} \cdot \tan^{-1}[\mathrm{B} \cdot \mathrm{x} - \mathrm{E} \cdot (\mathrm{B} \cdot \mathrm{x} - \tan^{-1}(\mathrm{B} \cdot \mathrm{x}))]\}, \quad (8)$$

where $\mathrm{Y} = \mathrm{y} + \mathrm{Sv}$, $\mathrm{X} = \mathrm{x} + \mathrm{Sh}$, being Y the output variable, i.e. the longitudinal force F_x or the lateral force F_y, and X the input variable, i.e. the longitudinal slip or the lateral slip (slip angle) (see also Fig. 3).

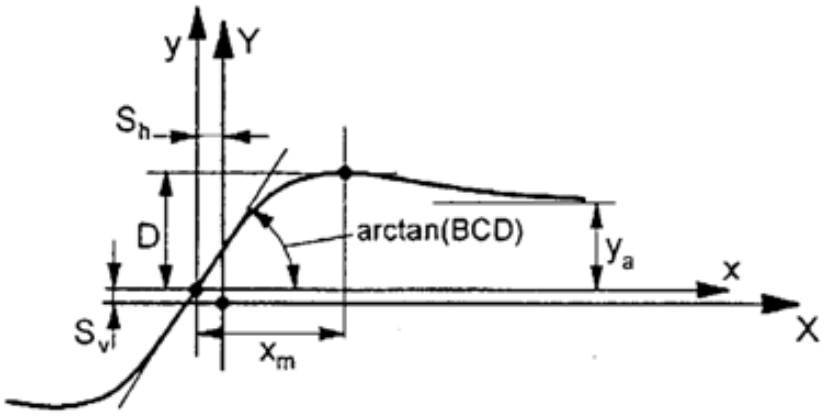

Fig. 3 Macro parameters of the magic formula**.**

In Fig. 4 the variations of Fy as a function of the the vertical load are shown.

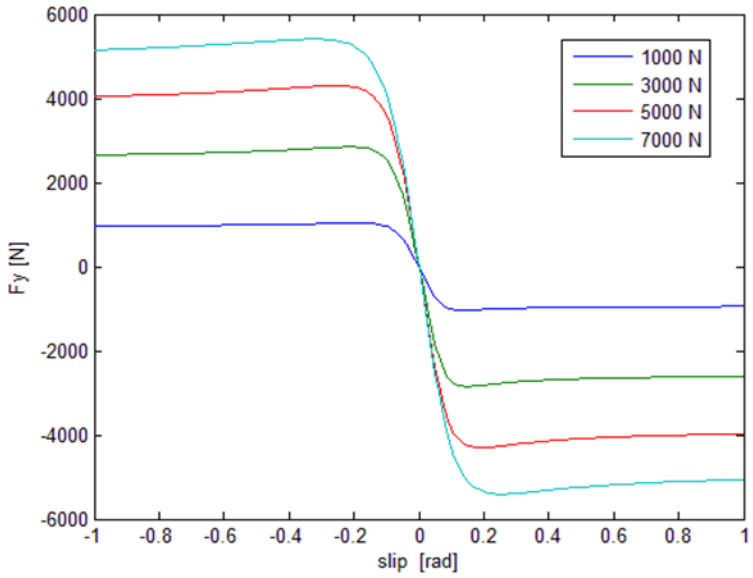

Fig. 4 Lateral force vations for various vertical loads.

2.3 Wheel and in-wheel motor models

By assuming a rigid wheel and by neglecting the rolling resistance, the wheel equation of motions is the following:

$$I_r \cdot \dot{\omega} = M - F_x \cdot R, \quad (9)$$

where M is the applied torque, I_r is the wheel inertia, and ω is the wheel angular velocity, F_x is the longitudinal interaction force, and R is the wheel radius.

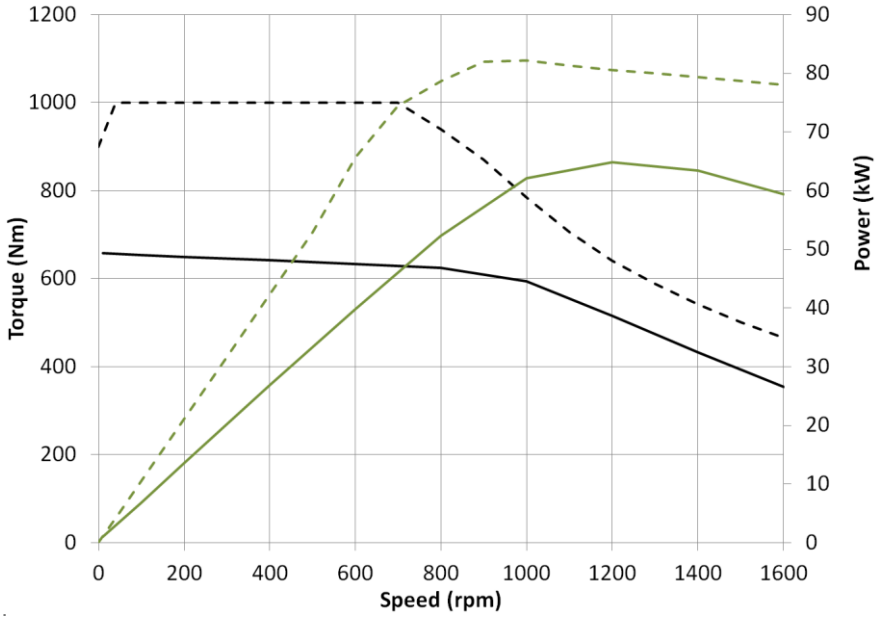

Fig. 5 Power and speed characteristic curves.

By neglecting the dynamics of the electric motor, a static nonlinear model is proposed, based on the power and speed characteristics of the motor (e.g., see Fig. 5).

3 Differential logics

In this Section, three types of differential logics are analyzed and compared. As a first case, the (ideal) *open differential* case is considered, where the engine torque is equally distributed, independently of the real conditions of the wheels. In Fig. 6, an example of a simulated open differential acting in presence of icy road conditions is reported.

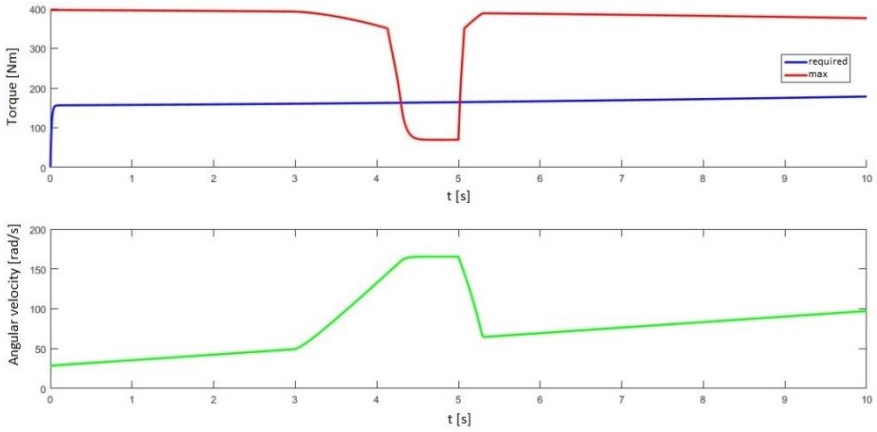

Fig. 6 Slip phenomenon with in-wheel motors**.**

A second case considered is the *speed-sensitive automatic locking* differential logic. A braking torque characteristic curve is now included in the model. Of course, the humping phenomenon previously shown in Fig. 6 does not occur since the braking torque suddenly goes to zero as soon as the velocity difference goes to zero.
Finally, a power sensitive automatic locking differential is analyzed. In this case it is assumed that the braking torque is linearly increasing with the input commanded torque. The slope of the curve is chosen considering that, as for the Torsen differential, the Torque Bias Ratio (TBR) is constant. The following relationship is adopted:
if $\omega_A > \omega_B$

$$M_A = \frac{M_P}{2} - M_f \tag{10}$$

$$M_B = \frac{M_P}{2} + M_f \tag{11}$$

since:

$$TBR = \frac{M_B}{M_A} \tag{12}$$

it is:

$$\frac{M_P}{2} + M_f = TBR \cdot \frac{M_P}{2} - TBR \cdot M_f \tag{13}$$

$$M_f = \frac{TBR-1}{1+TBR} \cdot \frac{M_P}{2} \tag{14}$$

By substituting (14) in (10)-(11), it follows:

$$M_B = \frac{TBR}{1+TBR} M_P \qquad M_A = \frac{1}{1+TBR} M_P \tag{15}$$

3 Simulation results

The mathematical model of the system components described above is implemented in a Matlab/Simulink^{TM} simulator. In Fig. 7 the main subsystems of the simulator are shown. Each part is characterized by a set tunable parameters and can be possibly modified independently.

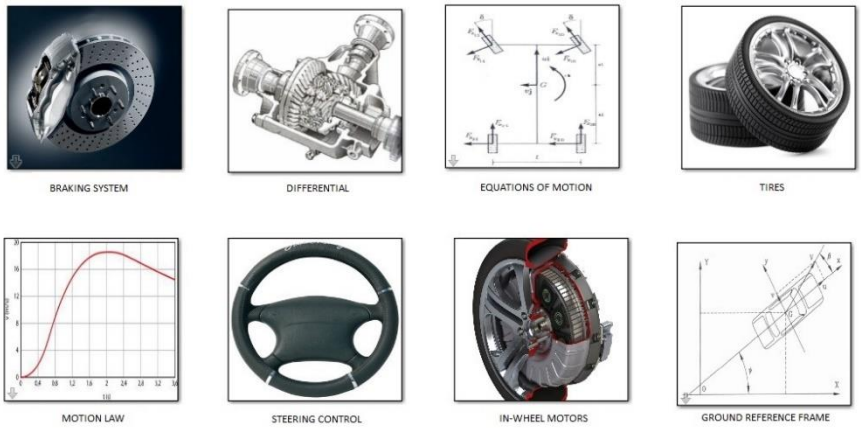

Fig. 7 Main subsystems of the electric vehicle simulator**.**

In Fig. 8, the speed sensitive and the power sensitive automatic locking differentials are compared in a maneuver on the straight where one of the two wheels encounters an ice floe. As it was expected, unlike the power sensitive differential, the speed sensitive differential provides appreciable torques only when the tire begins to slip.

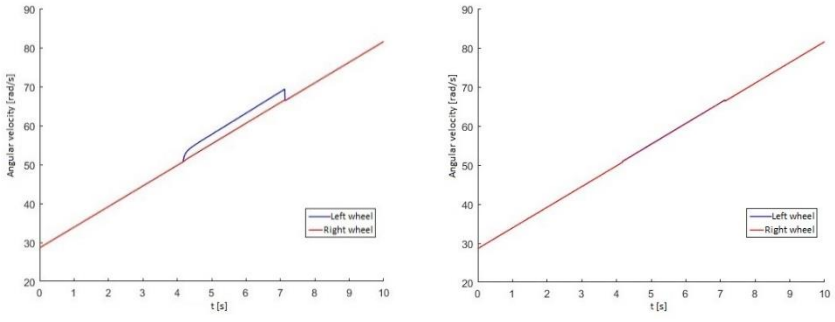

Fig. 8 Angular velocities with a speed sensitive (a) and a power sensitive (b) differential logics**.**

In the following simulation results, the open and the power sensitive differential logics are analyzed according to 4 different combinations:

- open central and axles differentials;
- open central and automatic locking axles differentials;
- automatic locking central and open axles differentials;
- automatic locking central and axles diffentials.

Each simulation assumes a TBR = 3 for the central differential, a TBR = 5 for the rear differential and a TBR = 2.5 for the front differential, which are typical values for a Torsen diffential. Three different maneuvers are used to make a performance comparison: a steering pad maneuver where the vehicle describes a circular trajectory with a radius of 100 m and a velocity growing from 30km/h with a constant acceleration of 2 m/s^2; an acceleration maneuver on straight from a starting velocity of 30 km/h and with a constant acceleration of 1.8 m/s^2, in presence of ice on the vehicle left side; an acceleration maneuver on straight from a starting velocity of 30 km/h and with a constant acceleration of 1.8 m/s^2, in presence of ice on both sides of the vehicle.

For the steering pad maneuver, the solution with both central and axles automatic locking differentials guarantees the best curvature (see Fig. 9). Moreover, the use of three automatic locking differentials provides the best roadholding (see Fig. 10).

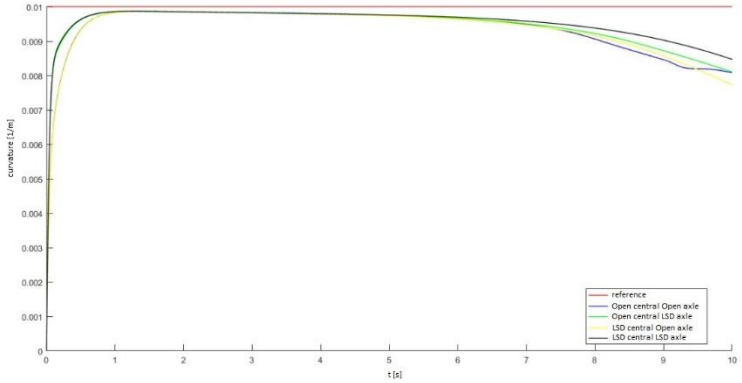

Fig. 9 Steering pad maneuver.

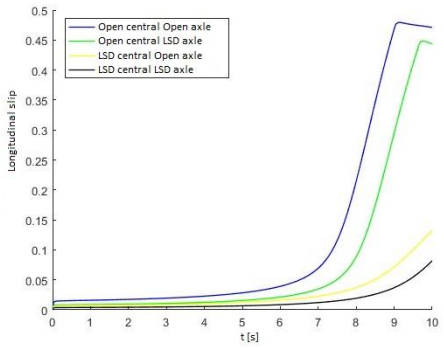

Fig. 10 Longitudinal slip of the front left wheel during the steering pad maneuver**.**

For the on straight constant acceleration maneuver, with icy conditions on the left wheels, the cases with open differentials and with automatic locking differentials are only reported. Again, the solution with only automatic locking differentials provides the best performance (see Figs. 11 and 12).

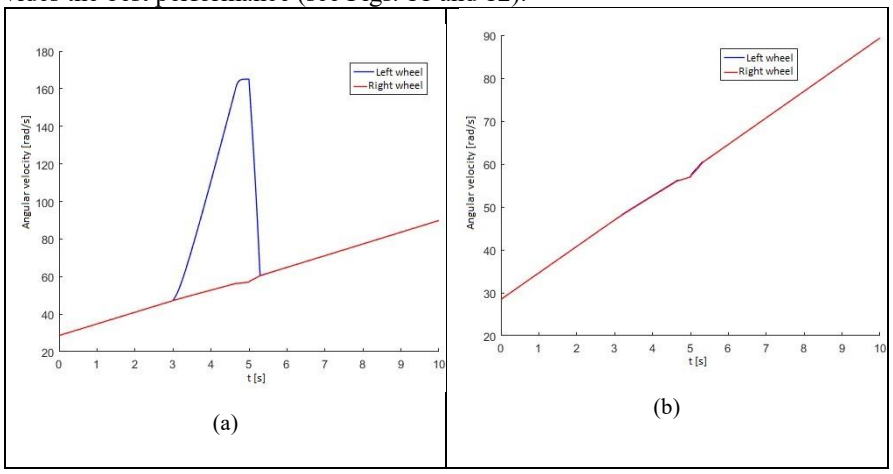

Fig. 11 Front (a) and rear (b) wheels angular velocities for an on straight acceleration maneuver with icy conditions on the left side of the vehicle and open differentials **.**

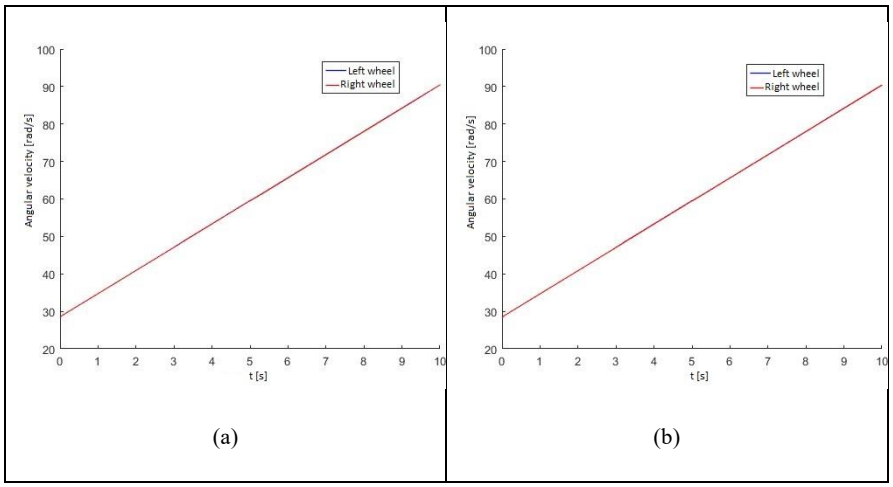

Fig. 12 Front (a) and rear (b) wheels angular velocities for an on straight acceleration maneuver with icy conditions on the left side of the vehicle and automatic locking differentials**.**

Similar results are obtained in last simulation scenario, i.e. an on straight constant acceleration maneuver with icy conditions on both sides of the vehicle. It is confirmed that the solution with central and axles automatic locking differentials guarantees the best performance.

4 Conclusions

In this paper the influence of the in-wheel motors on the vehicle dynamics has been analyzed. Starting from the mathematical model of the system components, a modular and parametric simulator has been developed in Matlab/Simulink™. The crucial problem of the torque distribution control among the 4 electric motors has been considered by evaluating various differential logics which mimic the currently employed ones. From the simulation results for the considered maneuvers, the best solution consists in adopting an automatic locking logic for both central and axles diffentials, which can be more easily implemented with respect to the internal combustion engines case. Possible future developments of this work could be the inclusion of an ESP control system with also a more complex car model for both the sprung and the unsprung masses and moreover the study of torque distribution logics not deriving from existing mechanical devices.

5 References

1. Chan, C. C., Bouscayrol, A. and Chen, K. 2010. Electric, hybrid, and fuel-cell vehicles: Architectures and modeling. IEEE Trans. Veh. Technol., 59: 589–598.
2. Rauh, J. and Ammon, D. 2011. System dynamics of electrified vehicles: Some facts, thoughts, and challenges. Veh. Syst. Dyn., 49: 1005–1020.
3. Hori, Y. 2004. Future vehicle driven by electricity and control – Research on four-wheel-motored UOT electric march II. IEEE Trans. Ind. Electron., 51: 954–962.
4. Murata, S. 2010. “Innovation by in-wheel-motor drive unit”. In UK Loughborough 10th International Symposium on Advanced Vehicle Control (AVEC)
5. Yan Chen and Junmin Wang - Design and Evaluation on Electric Differentials for Over-actuated Electric Ground Vehicles With Four Independent In-Wheel Motors - IEEE TRANSACTIONS ON VEHICULAR TECHNOLOGY, VOL. 61, NO. 4, MAY 2012
6. Iervolino R., Vasca F., Iannelli L. Cone-copositive piecewise quadratic lyapunov functions for conewise linear systems (2015) IEEE Transactions on Automatic Control, 60 (11), art. no. 7054477, pp. 3077-3082.
7. Celentano, G., Iervolino, R. Global modeling and simulation for analysis and design of a railway vehicle (2012) SPEEDAM 2012 - 21st International Symposium on Power Electronics, Electrical Drives, Automation and Motion, art. no. 6264492, pp. 1490-1495.
8. Sharifzadeh, M., Timpone, F., Farnam, A., Senatore, A., Akbari, A. - Tyre-road adherence conditions estimation for intelligent vehicle safety applications - 1st International Conference of IFToMM ITALY, IFIT 2016; Vicenza; Italy; 1- 2 December 2016, Mechanisms and Machine Science, Volume 47, 2017, Pages 491-501.
9. Russo, R., Terzo, M. , Timpone, F. Software-in-the-loop development and experimental testing of a semi-active magnetorheological coupling for 4WD on demand vehicles
10. Farroni, F., Russo, M., Russo, R., Timpone, F. (2014). A physical-analytical model for a real-time local grip estimation of tyre rubber in sliding contact with road asperities. Proceedings of the Institution of Mechanical Engineers, Part D: Journal of Automobile Engineering, Volume 228, Issue 8, July 2014, Pages 955-969. (DOI: 10.1177/0954407014521402).
11. M. Guiggiani, “Dinamica del veicolo”, ed. Città studi (1998).

12. H. B. Pacejka, “Tyre and vehicle dynamics”, Buttherworth Heinemann (2002).